Eur. Phys. J. Plus (2022) 137:1257
https://doi.org/10.1140/epjp/s13360-022-03473-1

THE EUROPEAN PHYSICAL JOURNAL PLUS

Regular Article

Forms and factors of deterioration of urban art murals under humid temperate climate; influence of environment and material properties

Teresa Rivas, Enrique M. Alonso-Villar[a], José S. Pozo-Antonio

CINTECX, GESSMin Group, Depto. De Enxeñaría dos Recursos Naturais e Medio Ambiente, Escola de Enxeñaría de Minas e Enerxía, Universidade de Vigo, 36310 Vigo, Spain

Received: 3 May 2022 / Accepted: 7 November 2022

Abstract This study describes the different alteration forms in 25 street art murals created between 2007 and 2018 on different substrates and located in different cities in NW Spain. The deterioration forms described affect the entire layer of the paintings as well as the substrates, with the most common being loss of colour (fading), loss of the pictorial layer -with or without loss of part of the substrate and biodeterioration. Physical, chemical, mineralogical and micromorphological analyses of samples from 10 murals revealed that (1) the deterioration mechanisms are related to environmental conditions and also to the inherent properties of the painting materials and to paint-substrate interaction, (2) the deterioration is closely associated with inherent aspects of urban art and (3) the loss of the pictorial record sometimes occurs in a very short period of time. The study findings highlight the need for preventive conservation measures in artworks (generally commissioned) that are intended to last.

1 Introduction

Today, art created in the public space constitutes, like the ancient cultural heritage, a very important part of the cultural legacy of communities. Ensuring its safeguarding through direct or indirect conservation interventions is essential to transmit to future generations all the artistic, cultural and sociological wealth of this type of artistic expression. However, contrary to what happens with ancient cultural heritage, knowledge about the deterioration factors that affect the stability of materials when they form part of or define urban art, especially pictorial art, is very limited, which negatively influences in its conservation and future transmission.

The different artworks included within the term urban art are created with a great variety of materials (wood, metal, paint etc.). The behaviour of these materials against the most common deterioration agents (water, gases, saline solutions and live organisms) are widely known in the case of ancient architectural and archaeological heritage, and the main forms of deterioration and alteration mechanisms affecting pictorial and stone cultural heritage are nowadays described [1–4]. Thus, thanks to the available knowledge on the deterioration processes, agents and forms, it is now possible to approach the conservation of restoration of ancient heritage monuments with the necessary scientific rigour.

However, knowledge about the deterioration processes that affect these materials when they form part or define urban art is very limited. Therefore, comparatively to ancient architectural heritage, scientific works focused on the diagnosis and conservation of real urban art materials are really scarce: only several studies about urban art on metal [5–7] and about pictorial urban art [8–12] are available.

One of the several reasons explaining this gap in knowledge could be the lack of consensus regarding the definition of urban art from artistic, social and, specially, legal points of view [13–15]. The lack of such a definition does not help in attempts to raise social and political awareness about urban art, which could lead to some commitment regarding conservation [16]; it also contributes to the lack of interest in the conservation of this type of art [13] which, from a practical point of view, greatly complicates the documentation and analysis of the artwork. The ephemeral nature of urban art also partly explains the lack of knowledge about the changes that occur in the materials involved: the conservation of the urban artworks is not of interest (or it is out of consideration) since their deterioration under the changing urban environment forms an intrinsic part of artwork itself [17–19].

Another possible reason for lack of knowledge on the deterioration of urban art materials is the complexity of the particular environment where urban artwork is created. The large variety of types of substrates (metal, wood, stone, concrete…), the incorporation of highly specific deterioration agents (derived from the specific climatology and the variety of anthropogenic activities defining the space), the techniques used to create the artworks—enormously conditioned by the context (environment)—and the constant modification of the urban space and its use by citizens together constitute new variables that define specific deterioration processes, which

[a] e-mail: enalonso@uvigo.es (corresponding author)

Published online: 19 November 2022

contribute to the ephemeral nature of this type of art [18]. In addition, ethical questions, derived from the involvement of multiple agents (artists, commissioning agents, local authorities, inhabitants of the urban space) must also be taken into account in defining conservation criteria [20]. With this level of complexity, it is impossible (and not recommended) to extrapolate the conservation protocols currently applied to ancient cultural heritage monuments to the specific case of urban art. Thus, restorer-conservators face problems regarding direct conservation measures, resolution of which has been deemed urgent [17].

Contemporary muralism is a type of artwork that has become popular in public spaces in recent years [18]. This type of artwork consists of murals, generally painted on the surfaces of fixed urban buildings and/or party walls, and commissioned by local authorities or other public entities, sometimes within the framework of festivals of urban art. The artistic creations within public spaces thus includes a wide range of artworks defined by, at one extreme, illegality and free expression [15] and at the other, by the more conventional exhibition circuit (contemporary muralism).

Although the conservation of painted artwork classified as independent is difficult for the reasons given above, in the case of contemporary muralism commissioned by local authorities, there appears to be some interest (at least by the commissioning authorities) in preserving of the artwork in the long term. In these cases, knowledge about the materials used in these urban artworks and how these materials interact with the different substrates under the particular environment is essential for determining measures that will slow down the deterioration of the artwork. Thus, in addition to scientific studies on the diagnose of real pictorial urban artworks already cited [8–12], the research about deterioration of materials used in urban art, especially paint degradation during different ageing tests, is arousing more and more interest [21–28]. The development of international research initiatives, such as the recent EU funding project CAPuS-Conservation of Art in Public Spaces [29] has promoted some of these recent scientific contributions and allowed the creation of the ideal interdisciplinary framework for the elaboration of a first draft of a glossary specifically devoted to pictorial urban art, the CAPuS glossary [30] which compiles terms related to cultural meaning, style and techniques of urban art and also proposes terms related to the deterioration and conservation specific to this type of artistic expression.

Despite this growing scientific interest in the subject, there is still a long way to go to gather enough scientific knowledge about pictorial urban art materials and their degradation to undertake rigorous conservation interventions, so more research is required in response to the increasing presence of this type of artwork in the public space.

The present work aims to increase knowledge about the state of conservation of pictorial urban art works under a humid temperate climate, describing, for the first time in the context of urban art in Spanish territory, the deterioration forms affecting materials and substrates of urban pictorial murals located in several cities of Galicia (north-west of Spain) characterized by different environmental conditions. The results of chemical, mineralogical and micromorphological analyses of the different deterioration forms of the murals allow us to define the deterioration mechanisms of the materials under humid temperate climate and, consequently, identify the most important alteration factors. This is an essential information to carry out a diagnosis of the conservation state of this type of artistic manifestation with a view to define a specific conservation protocol.

2 Materials and methods

2.1 Selection of the artworks

During the selection process, around one hundred murals were visited in the towns/cities of Vigo, Pontevedra, Ordes, Carballo and A Guarda (NW Spain); the artworks visited constitute a representative sample of the work of the artists currently active in Galicia and of the wide range of artistic styles defining urban art in Galicia, from the post-graffiti of the 1990s to the contemporary muralism [31, 32].

A total of 25 artworks (AW1 to AW25, listed in Table 1, Fig. 1) were selected from the total visited, considering variability in geography, type of substrate and conservation status. The authors of the 25 artworks were informed about the project and the interest in selecting their artworks, and in most cases, they granted permission to study and document the artwork. Basic information was compiled about the 25 artworks (location, orientation, distance from the sea, painting technique-brushing or spraying-, paint brand, substrate and any prior preparation). In each artwork, the deterioration forms affecting the substrate and the pictorial layer were described and their distribution on the artwork was reported. The ICOMOS-ISCS [3], EwaGlos [4] and CAPuS [30] glossaries were used for the description and nomenclature of the deterioration forms. Various of the authors also agree to be interviewed about their artworks (techniques, material, meaning); the interviews were conducted following the guidelines proposed by Cotte et al. [33]. The resulting conversations proved very valuable and the artists provided information about the social and economic context of their work and the main problems that arose during creation of the artworks.

2.2 Sampling and analysis

After consideration of the information compiled in the previous step, together with other factors such as the accessibility of each artwork, the substrate and the interest and participation of the artists and/or commissioning agents in conserving the artworks, 10 of them (AW16 to AW25) were selected for further study/analysis. Written permission was obtained from the artists for this part of the study. For each artwork, information about the artists and the artwork was recorded following the method proposed by Úbeda García

Table 1 List of the urban artworks selected for study of deterioration forms

ID	Author	Title	Year	Location	Structure	Substrate material	Paint application method	Underlayer	Deterioration forms
AW1	ANTONIO LAGUNA	Memoria sobre ladrillo	2011	Ordes	Party wall	Brick wall	Brush (TITAN) and spray	Yes	Fading
AW2	BLU	Untitled	2012	Ordes	Party wall	Brick wall	Brush (TITAN)	Yes	Fading
AW3	BOSOLLETTI	Untitled	2016	Ordes	Party wall	Rendered stone masonry and tiles	Brush (PROA) and spray	–	Biological growth, peeling, fading, abrasion, scaling, cracks
AW4	CESTOLA NA CACHOLA	Untitled	2016	Vigo	Surrounding wall of property	Concrete brick wall	–	–	Diffuse paint loss, biological growth, fading
AW5	CINTA VIDAL	Untitled	2007	Carballo	House facade	Cement-based rendered concrete brick wall, wood and metal	–	No	Diffuse paint loss, biological growth, fading, scaling
AW6	DELIO	Untitled	2012	Ordes	Party wall	Reinforced concrete	Brush (TITAN)	No	Biological growth, peeling, fading, abrasion
AW7	ESCIF	Extra calcium	2013	Ordes	Surrounding wall of farm	Rendered brick wall	Brush (PROA)	Yes	Diffuse loss, biological growth, fading, cracks
AW8	LIQEN	Buraco vermello	2010	Ordes	Party wall	Rendered stone masonry	Brush (TITAN)	Yes	Fading
AW9	LIQEN	Varrida	2012	Ordes	Party wall	Rendered stone masonry	Brush (TITAN)	Yes	Peeling, fading
AW10	PELUCAS	Untitled	2015	Vigo	Retaining wall	Stone masonry	Brush (EGA) and spray (MONTANA)	Yes	Diffuse loss, fading
AW11	PERI HELIO	Diógenes	2011	Ordes	Party wall	Rendered brick wall	Brush (EGA)	Yes (EGA)	Biological growth, peeling, fading
AW12	PERI HELIO	Génesis y Gnosos	2015	Vigo	Party wall	Rendered brick wall and reinforced concrete	Brush (EGA) and spray (MONTANA)	Yes (EGA)	Biological growth, peeling, fading
AW13	PERI HELIO	Ballena	2009	Cangas	Surrounding wall of factory	Concrete brick wall	Spray (MONTANA)	Yes (EGA)	Diffuse loss, biological growth, vandalism, peeling, abrasion, scaling, cracks, salt efflorescences
AW14	SEKONE	A mí me gustan los grafitis…	2013	Ordes	Party wall	Cement-based render on brick masonry	Brush (PROA) and sprays	No	Diffuse loss
AW15	SOKRAM	Untitled	2014	Carballo	Party wall	Brick wall and concrete columns	–	Yes	Fading, scaling

Table 1 continued

ID	Author	Title	Year	Location	Structure	Substrate material	Paint application method	Underlayer	Deterioration forms
AW16	DELIO	O lobo	2009	Pontevedra	Surrounding wall of property	Concrete brick wall	Brush	No	Diffuse paint loss, biological growth, vandalism
AW17	LIQEN	Entaraña	2008	Vigo	Surrounding wall of property	Rendered brick wall and reinforced concrete	–	No	Diffuse paint loss, biological growth, vandalism, peeling, fading, abrasion, scaling, cracks, craquelure
AW18	NOVE NOEL	Escarabajo pelotero	2012	Ordes	Wall surrounding a football pitch	Reinforced pre-cast concrete	Brush (TITAN)	No	Biological growth, peeling, fading, abrasion
AW19	SOKRAM	Pecado original	2012	Ordes	House facade	Rendered brick wall, wood, metal and concrete	Brush (TITAN)	Yes	Diffuse paint loss, biological growth, peeling, fading, scaling, salt efflorescences
AW20	SPOK	Minero asturiano de padre gallego	2015	Ordes	Wall surrounding a football pitch	Reinforced pre-cast concrete	Brush (PROA) and sprays	–	Biological growth, fading, craquelure
AW21	NUVI&EXFICO	A Guarda escrita nas estrelas	2018	A Guarda	Breakwater	Reinforced concrete	Spray (MONTANA)	Yes	Biological growth, peeling, fading, abrasion, scaling, cracks, superficial deposits, salt efflorescences
AW22	DOA OA	Reforestando artemisa vulgaris	2018	Carballo	Party wall	Cement-based rendered wall	Brush	Yes	Biological growth, fading
AW23	MOU	A Orixe 2	2018	Carballo	Party wall	Cement-based rendered brick wall, plastic and metal	Brush	Yes	Peeling, fading
AW24	LIDIA CAO	Xestando	2018	Ordes	Wall surrounding a football pitch	Reinforced concrete	Brush (PROA)	No	Peeling, fading
AW25	LIDIA CAO	Tempo	2018	Ordes	Wall surrounding a football pitch	Reinforced concrete	Spray (MONTANA)	No	Peeling, fading

An identification number (ID) was assigned to each artwork (AW). The name of the artist, title of the artwork, year of execution, location, type of structure on which the artwork was created, substrate material, paint brands (reported by the commissioning agents or the artists) and pre-treatments used (–: not provided) and type of deterioration forms are listed. Artworks 16–21 were selected for analysis of materials and deterioration forms and artworks 21–25 were selected for monitoring of colour changes over time

Fig. 1 Some of the artworks selected for this study. **a** Entaraña (AW17); **b** Pecado original (AW19); **c** Untitled (AW10); **d** Génesis y Gnosis (AW12); **e** A Guarda escrita nas estrelas (AW21); **f** Reforestando Artemisa Vulgaris (AW22); **g** A Orixe 2 (AW23); **h** Tempo (AW25)

[34]. The documented information included title, location, year of execution, type of structure, substrate material, artistic technique, paint brand, existence of an underlayer and state of conservation (deterioration forms). In addition, the extent of all deterioration forms was identified. Of the 10 artworks selected, 5 were painted before 2018 (AW16–20; AW17-Fig. 1a, AW19-Fig. 1b) and the other 5 were painted more recently, in 2018 (AW21–25; AW21-Fig. 1e, AW22 Fig. 1f, AW23-Fig. 1g, AW25-Fig. 1h).

Samples of the substrate material, the different deterioration forms and the unaffected pictorial layer were obtained in each of the 10 artworks selected (AW16–25). In addition, in the most recent ones (AW21–25) the deterioration was monitored by describing and photographing the state of the artwork, including the structure, the pictorial layer and the substrate, shortly after completion of the artworks (September 2018), one year later (December 2019) and two years later (December 2020). Thus, two samplings were carried out in these 5 artworks (AW21–25): (1) an initial sampling (September 2018) consisting of collecting samples of the substrates and surfaces painted with each type of paint used (considered as reference, undeteriorated samples) and (2) a second sampling, two years later (December 2020), in which samples of the pictorial surfaces were taken from the same points as in the first sampling and from areas affected by the different deterioration forms identified. In addition, the colour changes in the different paints used in

these 5 artworks (AW21–25) were monitored. Thus, areas painted in different colours were selected in each artwork, and the colour was measured by spectrophotometry. The spectrophotometer (Minolta CM-700d) was used in specular component excluded (SCE) mode, with a spot diameter of 3 mm, illuminant D65 and observer angle of 10°. Measurements were made at 10 random points in each area, and the mean values (and standard deviations) of the colorimetric coordinates in the CIELab and CIELCh spaces were calculated: lightness L^*, which ranges from 0 (black) to 100 (blank), a^* (positive values for red and negative values for green), b^* (positive values for yellow and negative values for blue), C^* (chrome) and h (hue). The initial colour values were used as reference data and in the same points, colour was measured every month for 18 months; in AW21 the first colour value was measured 5 months after completion of the artwork and every month for 10 months, with the final measurement made 28 months after the artwork was completed (i.e. 24 months after the first measurement). The colour change was quantified by calculating ΔL^*, Δa^*, Δb^*, ΔC^*_{ab}, ΔH^*, and the total colour change was calculated as ΔE^*_{ab} according to [35].

All of the samples collected were analysed using the following techniques:

(1) X-ray diffraction (XRD) (Siemens D5000 X-ray diffractometer), with Cu–Kα radiation and an Ni filter. The samples were analysed using the random powder method. Each mineral phase was identified using the X'Pert HighScore.
(2) Attenuated total reflection (ATR)-Fourier transform infrared spectroscopy (FTIR) (Spectrum 100 instrument with a diamond crystal—PerkinElmer, Weltham, Ma, USA). Each infrared (IR) spectrum was recorded at 4 cm^{-1} resolution over 16 scans ranging from 650 to 4000 cm^{-1}.
(3) Micromorphological analysis (Nikon SMZ1500). Both the surfaces of the samples and, in some cases, cross sections, prepared after embedding the samples in epoxy resin (EpoThin 2 Epoxy Resin and EpoThin 2 Epoxy Hardener) and polishing, were examined by this technique.
(4) Micromorphological and compositional analysis by means of scanning electron microscopy (SEM) with energy-dispersive X-ray spectrometry (EDS) (QUANTA 200 microscope), in both secondary electron (SE) and backscattered electron (BSE) detection modes. Observation conditions included a working distance of 10 mm, accelerating potential of 20 kV and specimen current of ~ 60 mA. The samples were studied by direct observation of the surface and, in some cases, cross sections were prepared as above.
(5) Soluble salt content was determined by high-performance liquid chromatography (HPLC) (ALLIANCE 2695 HPLC). For this analysis, 0.5 g (or a known weight) of the sample was shaken in 25 mL of deionized water for 1 h, after which the extract was filtered and the chloride (Cl^-), sulphate ($SO_4{}^{-2}$) and nitrate ($NO_3{}^-$) were determined.
(6) Scraped matter from the deteriorated areas of some artworks was observed directly and aqueous preparations of the matter were examined under an optical microscope (Nikon Eclipse 80i fluorescent microscope with NIS 80i software) to identify the different organisms present (algae, cyanobacteria, fungi).

3 Results and discussion

3.1 Location and description of the artworks

Information about the 25 artworks under study is compiled in Table 1. Most of the artworks selected for study are included within contemporary muralism, as defined by Gayo [18]; only 3 of them (AW5, AW13 and AW17-Fig. 1a) correspond to independent artistic manifestations within the Galician post-graffiti movement described by Romaní Fernández [31] and Arévalo [32]. All of the artworks were created between 2007 and 2018. Seven artworks (AW4, AW10-Fig. 1c, AW12-Fig. 1d, AW13, AW16, AW17-Fig. 1a and AW21-Fig. 1e) are located in coastal cities (Vigo, Pontevedra and Cangas); among these, five artworks (AW4, AW10, AW12, AW16 and AW17) are located at a distance of at least 2 km from the sea, and 2 artworks (AW13 and AW21) are painted on maritime structures (an old whaling station and a harbour wall) and are therefore in close contact with seawater and marine aerosols. The other artworks (18) are located inland in Galicia, in two rural populations characterized by intense agricultural and farming activity: Carballo (9.4 km from the sea) and Ordes (28 km from the sea).

In general, the climate to which all of the artworks are subjected is the characteristic climate of Galicia, which, according to the FAO agroecological zoning, corresponds to a humid subtropical climate, with rainy winters (1180 mm weighted average annual rainfall) and average annual temperature of 15 °C [36, 37]. Following the Köppen–Geiger climate classification system, the region has an oceanic type Cfb climate [38] and is therefore enormously influenced by oceanic masses (the Atlantic Ocean in the west and north and the Cantabrian Sea in the north) and by the orography. So, areas close to the coast are characterized by a hyperoceanic climate with an annual mean temperature of 14–15 °C, low thermal amplitude (i.e. the difference between the mean temperature in the coldest and the hottest months) (less than 12.5 °C) and high rainfall, especially on the Atlantic coast. As the distance from the coast increases, the annual mean temperature and the relative humidity both decrease and the thermal amplitude increases. The coastal locations (Vigo, A Guarda, Pontevedra and Cangas) and the inland locations (Carballo and Ordes) are not very far apart. However, (1) the precipitation varies widely, with annual values varying widely, between 1600–1800 mm (A Guarda, Vigo), 1400–1600 mm (Ordes), 1200–1400 mm (Pontevedra and Cangas) and 1000–1200 mm (Carballo); (2) in all of the locations the

annual mean temperature varies between 13 and 15 °C, although the thermal amplitude in interior locations (Ordes and Carballo) is slightly higher (13.5–14.5 °C) than in coastal locations (< 12.5 °C) [37].

The artworks have been created on various types of civil/urban structures. Most are painted on walls of private buildings: 12 on party walls of buildings of between 2 and 6 floors (Fig. 1d, f, g), 2 on exterior walls of factories, 3 on perimeter walls of private urban plots and 2 directly on the facades of individual houses (Fig. 1b). The remaining 6 artworks are painted on structures owned by different authorities: AW21 (Fig. 1e) covers the length of the breakwater wall of the A Guarda harbour (240 m), AW10 (Fig. 1c) covers the surface of a retaining wall of height 16 m and width 8 m, and the other 4 artworks (including AW24, Fig. 1h) are painted on perimeter walls of football grounds owned by local authorities. All of the artworks are accessible (up to a height of a least 2 m) to the public and animals.

The substrates are varied, including unrendered brickwork (3 artworks) and rendered brickwork (9 artworks), which is usually coated with cement and aerial lime concrete. Several of the artworks are also painted on unrendered reinforced concrete (6 artworks) or on unrendered concrete blocks (3 artworks). Four of the artworks are painted on natural stone masonry walls covered with cement and aerial lime concrete, and in another 4 artworks (including those painted on house walls) the paint also covers metal, plastic and wooden structural components.

The substrates were only preconditioned before being painted in 11 of the artworks, all of which are commissioned by local authorities and painted on the retaining walls of buildings (6 artworks) or on the walls of public buildings (3 artworks). In most cases, the conditioning consisted of the application of a layer of white exterior paint; in only three artworks (all painted by the same artist) the conditioner was specifically intended for use on outdoor facades (water based acrylic resin coatings from EGA).

Information about application or execution technique was only obtained for 21 of the artworks: in 12 artworks the paint was applied with a brush; in 6 the paint was applied using a mixture of brush and spray techniques; and only 3 were spray painted. The commercial brand of the paint is known for most (18) of the artworks: TITAN, EGA and PROA for brush application and MONTANA for spray application.

More detailed information is available on the substrate and the paint materials used in AW21, which was examined over a period of 2 years to monitor the state of conservation (Fig. 1e). This artwork was painted on the main breakwater that partly encloses the natural harbour at A Guarda (SW Galicia), an open bay of length 564 m and width 260 m. The breakwater, built from reinforced concrete, extends south from the northern side of the harbour (direction S28W) and is of length 240 m and height 8 m. It comprises a stepped structure (2 or 3 steps) constructed from 2 or 3 reinforced concrete rectangle modules (Fig. 1e). In 2011, the inner (sea protected) side of the breakwater was first painted by Eduardo Zamarro but, in 2017, part of the structure collapsed during a severe sea storm. In 2018, after the reconstruction, a blue acrylic paint (Montokril acrylic paint, S 5540r90b) was sprayed along all the inner side of the breakwater (covering the remains of the previous Zamarro's artwork) and the current AW21 artwork (Fig. 1e) was painted on it. AW21 artwork was created by stencil technique on the blue painted surface, by painting numerous figures in six different Montana Colours MNT 94 spray paint colours: light yellow (RV-1021), blue (RV-151), safari brown (RV-135), orange (RV-2004), valley green (RV-6018) and pink (RV-115).

3.2 Forms of alteration and mechanisms of deterioration

All of the artworks display some level of deterioration, including the most recently created artworks (Table 1). The types of deterioration identified were decolouration (fading), various conditions leading to loss of the pictorial surface (scaling, diffuse loss, peeling and craquelure), biological colonization, cracks and fissures, surface deposits (including salt efflorescences), abrasion and overpainting (vandalism).

Next, the different deterioration forms, their presence and distribution in the artworks and the mechanisms involved on their formation are described in more detail, based on the results obtained from the analysis of the samples collected.

3.2.1 Decolouration (fading)

Fading is the most common deterioration form, affecting 22 of the 25 artworks. The pictorial layer is (apparently) physically intact, but has undergone a visible colour change towards whitish/greyish faded tones (Fig. 2a, b). No clear relationship was observed between the presence and intensity of this type of alteration and the degree of exposure of the murals to direct sunlight; there was also no apparent relationship between the intensity of the fading and the type of the substrate, as it affected paintings on both rendered and unrendered brick and concrete surfaces (Table 1). In some of the artworks (AW18 and AW20: Fig. 2a, b), the loss of colour is so intense that only grey tones are observed.

Fading can occur quite rapidly, as observed during monitoring of the deterioration of AW21. In this artwork, a clear relationship was also observed between the colour of the paint and the rate at which it faded: the pink and orange paints had visibly faded 12 months after completion of the artwork and the fading was even more intense after 24 months (Fig. 2c–e), while the colour of the blue, yellow and green paints was scarcely altered (Fig. 2f–h).

The relationship between the intensity of fading and the paint colour was also revealed by the colorimetric measurements carried out in this mural (AW21) and the other 4 murals created in 2018 (AW22-AW25, Table 1). The variations in the global colour change ΔE^*_{ab} in selected areas of AW21, AW22, AW24 and AW25 during the monitoring period are represented in Fig. 3. The detailed

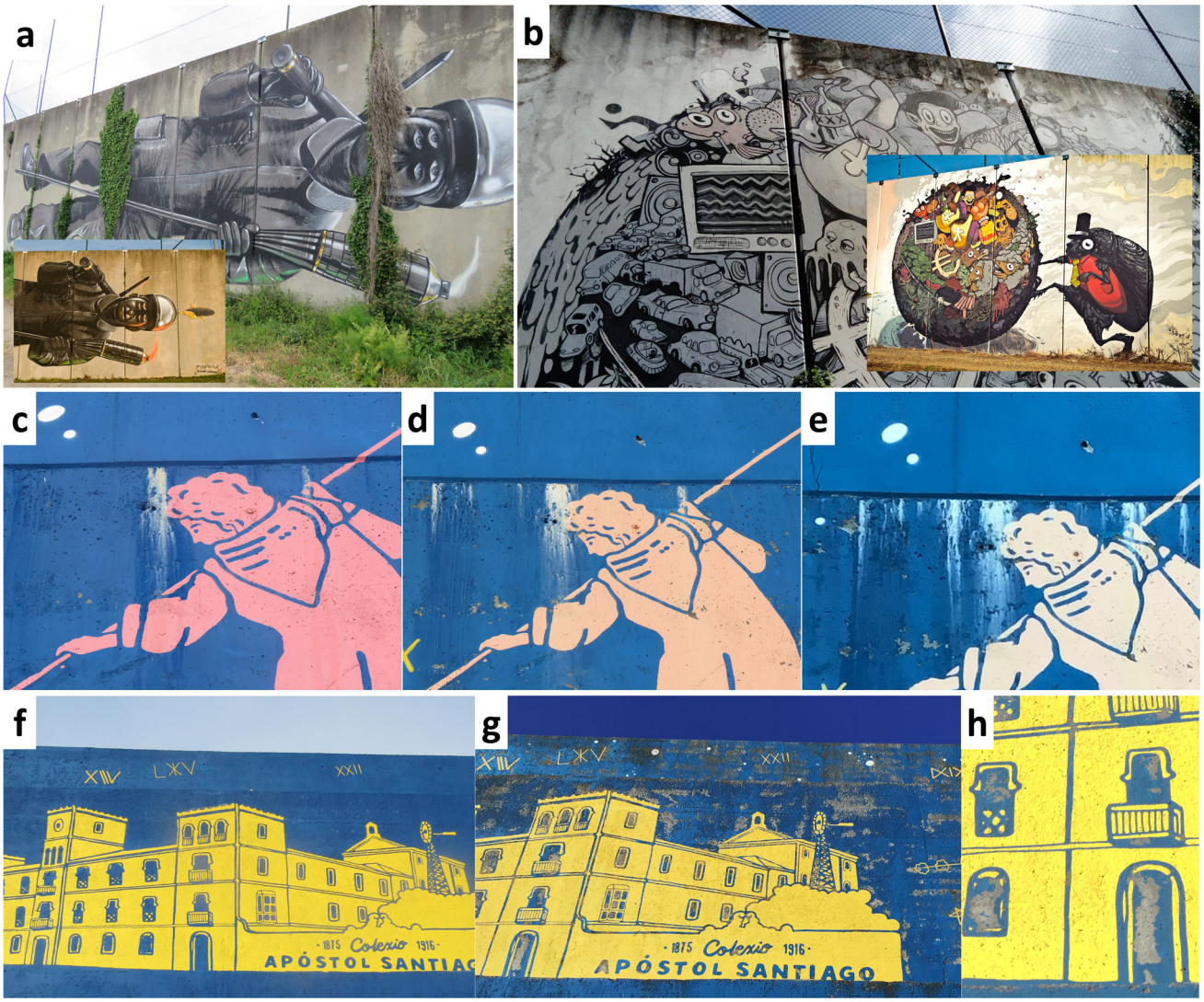

Fig. 2 Fading affecting AW20 (**a**), AW18 (**b**) and AW21 (**c–h**) artworks; **c–e** images of a detail of a pink-painted iconography from AW21 taken in 2018 (**c**), 2019 (**d**) and 2020 (**e**); **d–f** images of a detail of a yellow-painted iconography over the blue base paint of AW21, showing the progression of the deterioration from 2018 (**f**) to 2020 (**g** and **h**)

examination of the variations of this parameter over time and of the absolute values reached at the end of the monitoring period reveal the following:

(1) The magnitude of ΔE^*_{ab} varied in relation to the *hue*. In order to discuss the changes in this colorimetric parameter, a threshold value of 3.5 CIELab units, above which a chromatic change is visible to an unexperienced eye [39], is considered. If the variation of ΔE^*_{ab} of the painted areas of the AW21 (Fig. 3a) and that of AW22 (Fig. 3b) artworks are compared, it can be seen that pink and orange colours already exceeded the threshold of $\Delta E^*_{ab} = 3.5$ CIELab units from the 6th–8th month after execution, whereas ΔE^*_{ab} for green and blue tones remained lower for longer. Likewise, the final values of ΔE^*_{ab} were always lower for green and blue tones than for orange, pink and yellow paints, which reached extraordinarily high values: ΔE^*_{ab} 16.1 CIELab units (month 14) in the orange paint in AW21 (Fig. 3a), ΔE^*_{ab} of 17 CIELab units (month 14) in the pink paint in AW21 (Fig. 3a) and 7.7 and 4.7 CIELab units in, respectively, the dark and light pink paint in AW22 (Fig. 3b).

(2) The magnitude of ΔE^*_{ab} seemed to vary with the lightness of the paints. So, comparing data of AW22 and AW25 artworks (Fig. 3b, d), in which colour changes in paints of the same chroma but of varying degrees of lightness (i.e. different *value)* were evaluated, it can be seen that ΔE^*_{ab} values were always higher in the darker green, violet and brown colorations (dark green-DG, deep violet-DV and dark brown-DB) than in the lighter colorations (LG-light green, LB-light brown and LV-pale violet); the only exception to this pattern was the pink paint in AW22: at the end of the study period (month 9–13) the ΔE^*_{ab} value for the lighter colorations (LP-light pink) was slightly higher than for the darker pink paint. In AW23 artwork (data not shown), it was also confirmed that the darkest blue colours of this work (Fig. 1g) reached values of ΔE^*_{ab} higher, both during

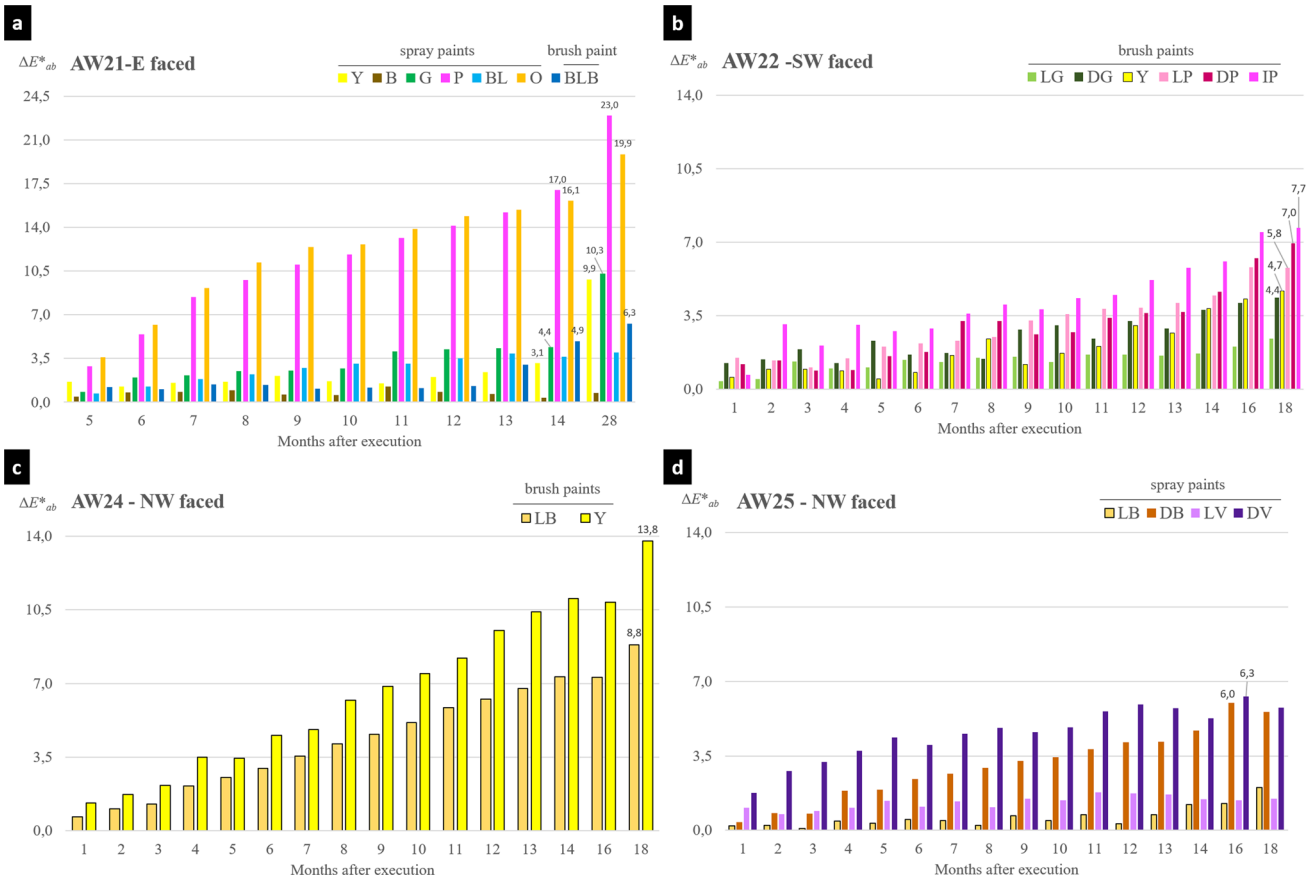

Fig. 3 Variation of the ΔE^*_{ab} over time (months from the execution of the artwork) in areas painted with different colours selected in AW21 (**a**), AW22 (**b**), AW24 (**c**) and AW25 (**d**) artworks. The monitored colours are as follows: AW 21—yellow Y, brown B, green G, pink P, blue BL, blue paint base BLB; AW 22—light green LG, dark green DG, yellow Y, light pink LP, dark pink DP, intense pink IP; AW 24—light brown LB, yellow Y; AW 25—light brown LB, dark brown DB, light violet LV, dark violet DV. The orientation of the mural and the type of paint used in each artwork (spray or brush-type) are also indicated. Note the different *y*-axis scale of AW21 graph, respectively, to the other graphs

the monitoring period and at the end of it: thus, the ΔE^*_{ab} of the darkest blue of this artwork was 2.31 CIELab units and the ΔE^*_{ab} of the lightest blue of this artwork was 1.32 CIELab units.

(3) The non-existence of a clear relationship between the ΔE^*_{ab} value reached at the end of the monitoring period and the geographical orientation of the walls on which the artworks were painted (orientation shown in Fig. 3). Of all the artworks, AW22 (Fig. 3b), which faces SW, receives the greatest number of hours of sunlight; however, the ΔE^*_{ab} values for the paints examined in this artwork were similar to those reached in AW 24 (Fig. 3c) and AW25 (Fig. 3d) artworks whose orientation (NW faced) supposes fewer hours of sunlight.

(4) The way in which ΔE^*_{ab} changed over time was different among artworks and, within each artwork, among the different colours monitored. In some cases, the ΔE^*_{ab} increased gradually from the first month of study, as observed in the yellow and brown paints in AW24 (Fig. 3c); in other cases, such as the brown paint in AW21 (Fig. 3a, B paint), the light brown paint in AW25 (Fig. 3d, LB paint) and almost all the colours in AW22 (Fig. 3b), the ΔE^*_{ab} values fluctuated throughout the period with no clear pattern of variation. In AW25 (Fig. 3d), the ΔE^*_{ab} values in the pale violet (LV), deep violet (DV) and dark brown (DB) increased gradually from the start of the study, but then changed more slowly, after, respectively, 6, 10 and 14 months. The opposite seems to have happened in AW21 (Fig. 3a), where ΔE^*_{ab} increased more rapidly during the first 8 months after completion of the artwork, after which the colour faded gradually and more slowly; interestingly, during the 14 months between the last two measurements (i.e. at 14 months and 28 months) the ΔE^*_{ab} in the least resistant paints (pink-P and orange-O) only increased by between 4 and 5 units, which is much lower than the increases of 17 and 16 units that occurred during the first 14 months of study.

No relationship was observed between the variations in ΔE^*_{ab} during the study period and the meteorological season; the periods when the ΔE^*_{ab} changed more slowly or displayed lower values did not coincide with seasons when the number of daylight hours is lowest (end of autumn, winter and beginning of spring, which, in Galicia, coincide with periods of heaviest rainfall). Alonso-Villar et al. [27] reported that the variation in ΔE^*_{ab} during prolonged exposure to ultraviolet (UV) radiation was not linear, and in some cases, variations occurred even when the level of UV radiation remained constant. It is possible that in the murals considered in the

present study, colour changes caused by solar radiation are added to probable occasional colour changes related to the substrate (e.g. due to the moisture content, especially in winter and spring) or to the presence of dust deposits on the surface (which may contribute to colour changes during summer).

Analysis of the contribution of each colorimetric coordinate to the ΔE^*_{ab} showed that in general, the ΔE^*_{ab} suffered by the paints under study was due to an increase in L^* and a decrease in C^*, changes that are qualitatively associated with loss of colour saturation, so that the paint becomes lighter in colour. The term used to describe this type of alteration, i.e. fading, refers to this loss of the colour intensity. However, several exceptions were observed: (1) in the brown (B) paint in AW21 and yellow (Y) paint in AW22, the values of the L^*coordinate and the C^* coordinate decreased slightly, causing darkening of the colour. However, although the original colour did not become lighter, loss of saturation occurred, as the C^* decreased, leading to greyish colouration; (2) the cobalt blue undercoat (BLB) in AW21, and both shades of violet (LV and DV) and the dark brown (DB) paints in AW25 underwent increases in L^* and in C^*, although there was no loss of saturation (or purity) of these colours.

Analysis of the paint samples collected before and after the monitoring period confirmed that the colour changes were not due to mineralogical alterations. The mineralogical compositions of some of the samples taken from artworks affected by fading and of the reference samples from the same artworks are shown in Table 2. In the reference (not deteriorated) paint samples, inorganic phases such as titanium oxide (TiO_2) and calcite ($CaCO_3$) (commonly used as fillers and opacifiers) were observed. In the samples of paint affected by fading, the same mineral phases identified in the unaltered paints were detected; neoformed minerals or exogenous compounds such as soluble salts were not detected in any of the samples. However, comparison of the FTIR spectra of paint samples from AW21 immediately after completion of the artwork and one year later revealed changes in the functional groups in the organic fraction; Fig. 4 depicts, as an example, the FTIR spectra of the orange spray paint in AW21 at those two moments. The FTIR spectra of the reference paints confirmed the alkyd nature of the spray paints used in this work by means the identification of the typical fingerprints of alkyd paints: O–H stretching vibration between 3430 and 3300 cm^{-1}, the typical doublet at 2922–2851 cm^{-1} assigned to the stretching vibration of the C–H group, the C=O carbonyl stretching at 1720 cm^{-1}, the C–O–C ester at 1254 cm^{-1} and C–H in the plane bending doublet 1114–1066 cm^{-1} [21, 22, 40, 41]. After one year of environmental exposure, the intensity of the C=O carbonyl band stretching at 1720 cm^{-1} decreased (Fig. 4), indicating partial loss of carbonyl groups from the polymer [42–44]. A decrease was also observed in the intensity of the doublet 2922–2851 cm^{-1} characteristic of stretching vibration of the C-H group, indicating hydrogen abstraction processes associated with destruction of the backbone structure of the polymer [42, 43]. The 3430–3300 cm^{-1} band of the O–H group also decreased after environmental exposure, which is surprising given that the organic polymers become degraded by oxidation processes with the consequent increase in this band. However, in a previous study analysing the degradation of spray paint in this artwork (AW21) exposed to UV radiation [27], the reduction in intensity of this band after exposure was related to the triggering of reactions between radicals and free O–H groups during the degradation process. The fact that the band at 1720 cm^{-1} (C=O carbonyl group) was not displaced towards higher or lower wavelengths rules out the formation of ketones or lactones as a result of the reaction between free OH radicals [42–45] and indicates the possibility that the products of these first reactions (of lower molecular weight) have been lost by volatilization. The reduction in the intensity of the 1114–1066 cm^{-1} C–H doublet in plane bending supports this hypothesis.

Taking the above results into consideration and in accordance with previous findings [22–24, 27, 42, 43, 46–51], the fading observed in the artworks under study can be attributed to the effects of UV radiation on the organic polymers contained in the paints (i.e. binders or chromophores). The observed differences between the artworks under study in regard to the intensity of fading is probably due to the different paint formulations. It is also possible that the substrate influenced the colour changes in the paints. Alonso-Villar et al. [27] reported that minimal loss of adherence between the paint and substrate (favoured by the type of substrate, e.g. by smooth substrates such as brick and pre-cast concrete, or by the paint formulation) may lead to changes in the perceived colour, although the loss of adherence does not represent a risk of loss of the pictorial layer.

3.2.2 Loss of pictorial layer: scaling, diffuse loss of material, peeling and craquelure

Four types of deterioration were distinguished, all of which caused loss of the pictorial register and of the paint layer:

(1) *Scaling*. Detachment of the pictorial layer along with substrate material (Fig. 5a). In 7 of the artworks, scaling caused centimetre-scale gaps whereas in another 9 artworks the peeling generated millimetre-sized gaps defined, in this study, as diffuse loss (Fig. 5b).

The artworks affected by scaling were those painted on walls made of reinforced concrete, concrete bricks or bricks (but, in the latter, only on bricks rendered with a cement-based render). Examination of the artworks affected appears to indicate a relationship between the development of scaling and the state of conservation and/or characteristics of the substrate. In two of the artworks (AW13 and AW19), the scaling appeared to be related to the presence of salt efflorescences, and in AW20, to defects in the concrete (Fig. 5c).

The mineralogical composition of the samples of scaling from the two artworks most affected by this type of alteration, i.e. AW19 (painted on a brick wall coated with a cement-based render, Figs. 1b and 5a) and AW20 (painted on a reinforced concrete wall, Figs. 2a and 5c) is shown in Table 2. In all samples, variable amounts of calcite and silicates, mainly quartz (SiO_2), although also smaller quantities of muscovite, feldspar and chlorite were detected. These phases mainly correspond to the aggregate and the

Table 2 Mineralogical composition determined by X-ray diffraction analysis (semiquantitative results) of (1) samples of several colours of paints immediately after completion of the artwork (in 2018) and after 24 months (in 2020) affected by fading, (2) scaling samples, (3) undeteriorated concrete and rendered substrates; (4) peeling samples and (5) surface deposits

Sample	Description	C	Q	Pl	KF	M	Cl	T	R	P	G	Others	Cl^-	$NO_3{}^-$	$SO_4{}^{-2}$
AW21-SP18	Reference pink paintwork (2018)	***							**				n.d	n.d	n.d
AW21-FSP20	Faded pink paintwork (2020)	***							**				n.d	n.d	n.d
AW21-SO18	Reference orange paintwork (2018)	****							***				n.d	n.d	n.d
AW21-FSO20	Faded orange paintwork (2020)	***	*						**				n.d	n.d	n.d
AW19-S1A	Scaling affecting support	*	****		*		*						92.05	729.71	301.93
AW19-S2A	Scaling affecting support	*	****		*		*						86.78	1050.92	1066.01
AW19-SV1	Scaling affecting green paintwork + support	**	***	tr									58.77	527.25	140.89
AW19-SV2	Scaling affecting green paintwork + support	**	***	tr		tr	tr						58.35	533.73	80.17
AW19-S3	Scaling affecting white paintwork g + support	**	*					*	**		**		103.65	250.95	22,879.41
AW20-S1	Scaling affecting reinforced concrete	**	***	tr								tr-Ettringite	n.d	n.d	n.d
AW17-B1	Diffuse loss affecting grey paintwork	***	***						*				n.d	n.d	n.d
AW17-S	Diffuse loss affecting paintwork and support	*	****	tr	tr	tr			tr				n.d	n.d	n.d
AW16-N	Diffuse loss affecting black paintwork	****	tr					*	*				n.d	n.d	n.d
AW16-A	Diffuse loss affecting yellow paintwork	****						tr	*				n.d	n.d	n.d
AW16-S	Concrete brick	**	***	*	*	*	tr						10.11	46.49	22.08
AW21-PR	Peeling (pink paintwork)	***							***			tr-Halite and Epsomite	447.06	16.18	97.06
AW21-PBlB18	Peeling (blue base paintwork) 2018	***						**	tr			tr-Halite, Epsomite and Thenardite	228.75	23.75	50.00
AW21-PBlB19	Peeling (blue base paintwork) 2019	***						**	tr			tr-Halite, Epsomite and Thenardite	205.88	19.12	35.78
AW21-H1	Original concrete	**	****							tr			796.45	1.31	89.21
AW21-H2	Reposition concrete	****	*	tr	tr								92.93	1.54	21.89
AW21-P	White deposit (2018)	****	tr	tr	tr								n.d	n.d	n.d
AW21-A2	White deposit in fissure (2019)	****										tr-Epsomite and Thenardite	n.d	n.d	n.d
AW21-A1	White deposit associated with infiltration	***	*	*		*						**-Mg $(OH)_2$	n.d	n.d	n.d
AW21-BlB18	Reference blue base paintwork (2018)	***					tr	**					n.d	n.d	n.d
AW21-FBlB20	Whitened blue base paintwork (2020)	***					tr	**				tr-$(Ca,Mg)CO_3$	n.d	n.d	n.d

The dissolved ion content (mg ion/100 g sample) is also shown for several samples

C—Calcite, *Q*—quartz, *Pl*—plagioclase, *KF*—potassium feldspar, *M*—muscovite, *Cl*—chlorite, *T*—talc, *R*—rutile, *P*—Portlandite, *G*—gypsum, Cl^-—chloride, $NO_3{}^-$—nitrate, $SO_4{}^{2-}$—sulphate

**** >50%; ***30–50%; **10–30%; *3–10%; tr: <3%

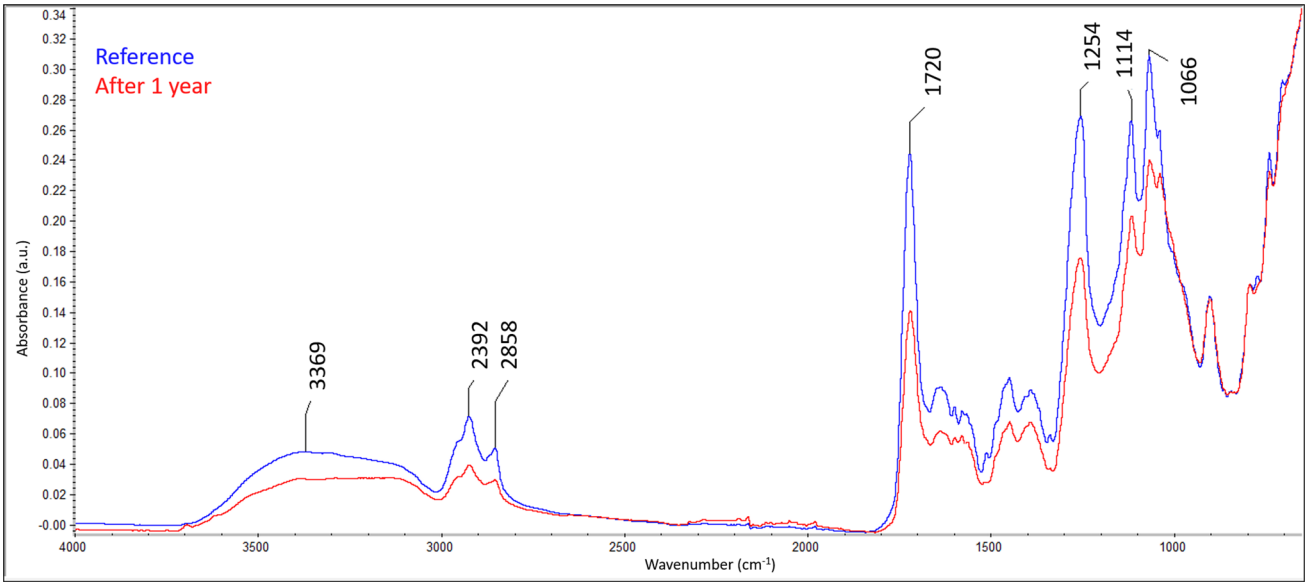

Fig. 4 FTIR spectra of a sample of orange paint from AW 21 collected immediately after the execution of the work (2018) and of a paint sample of the same colour taken one year later

cement phases of the render substrate, as will be described below. In a sample of scaling affecting the white paint in AW19 (Figs. 1b and 5a), paint components such as talc (between 3 and 10%, used as filler) and rutile (between 10 and 30%, used as filler, although in this case corresponding to the white pigment), were identified. Large amounts of gypsum –$CaSO_4{\cdot}2H_2O$– (10–20%) were also detected in the same sample. Soluble salts were also extracted from all of the scaling sample: data summarized in Table 2 show that the sulphate ion content was very high (up to 22 g per 100 g of sample) in the scaling sample from the white paint, in which XRD analysis revealed the presence of gypsum. Large quantities of soluble ions were also detected in the other samples from the same artwork, including nitrate (Table 2, samples S1A and S2A) and sulphate (Table 2, sample S2A). During the visual inspection of AW19 (Figs. 1b and 5a), abundant salt efflorescences were observed in some areas close to the base of the facade on which this artwork is painted. Part of this facade wall bridges a small river, which could be a source of salts; dissolved salts from the water would rise up the wall of the façade via capillary action crystallizing as efflorescence. It is very likely that nitrate (very abundant in these samples) comes from this river since this artwork is located in a rural environment where there are numerous agricultural and livestock farms. On other hand, ettringite ($Ca_6Al_2(SO_4)_3(OH)_{12}{\cdot}26H_2O$) was detected in the scaling sample from AW20 (Figs. 2a and 5c); ettringite is a secondary sulphate mineral formed during chemical deterioration of concrete due to the sulphate reaction [52]. The origin of the sulphate is more uncertain; it is possible that it comes from the construction materials, as pointed out in other researches on the origin of sulphated salts in monuments [53, 54], although contributions from the river, related to the use of pesticides, and from marine aerosol [55] have not been ruled out.

SEM analysis of the samples affected by scaling in AW19 and AW20 support the hypothesis that the scaling is due to the action of salts. Thus, the presence of ettringite in the sample from AW20 was confirmed by the detection of the typically fibrous deposits of this salt (Fig. 5d). Analysis of the samples from AW19 revealed that the nature and size of the aggregate grains of the rendering mortar vary greatly throughout the entire facade. Thus, in some zones (e.g. where samples SV1 and SV2 were collected, Table 2), aggregate of the rendering mortar consist on angular grains of quartz and feldspar (Fig. 5e), while in other areas of the facade, the aggregate consists on rounded grains mixed composition, of silicate nature (quartz, feldspar and mica grains) and biogenic nature; the presence of rounded fragments of mollusc shells (Fig. 5f) may indicate the use fluvial sediments (or coastal sediments, as the distance from the sea is about only 15 km). In the same samples, the cement phase of the rendering mortar is rich in Ca, O and C, elements which form calcite (confirming the XRD data), indicating complete carbonation of the portlandite. In addition, the use of Portland cement is confirmed by means the detection of aggregates rich in Ca and Si (Fig. 5f), which correspond to residual non-hydrated cement phases, and Si, Ca and O rich aggregates identified as calcium silicate hydrate (C–S–H) phases [56]. The micrographs reveal that the mortar is affected by long fissures, which surprisingly appear to affect only the mortar and not the pictorial layer (Fig. 5e). This observation suggests that the rendering mortar was already deteriorated before the paint was applied. On the other hand, SEM–EDS analysis revealed the systematic presence of S and Cl in the samples. Thus, the very poor cohesion of the mortar observed by SEM, together with the S and Cl detected by SEM–EDS and the detection of high contents of dissolved ions (Table 2) seems to confirm that the scaling, in this case, is caused by processes related to the presence of soluble salts of exogenous origin, which, through alternating processes of crystallization and dissolution, disaggregate the mortar (causing fissures and fractures) and cause it to fall, dragging the paint layer with it. The disaggregating action of the salts by crystallization-dissolution processes is considered one of the deterioration mechanisms that affect concrete stability [57–59]; moreover, sulphate and chloride ions are salts of marine origin,

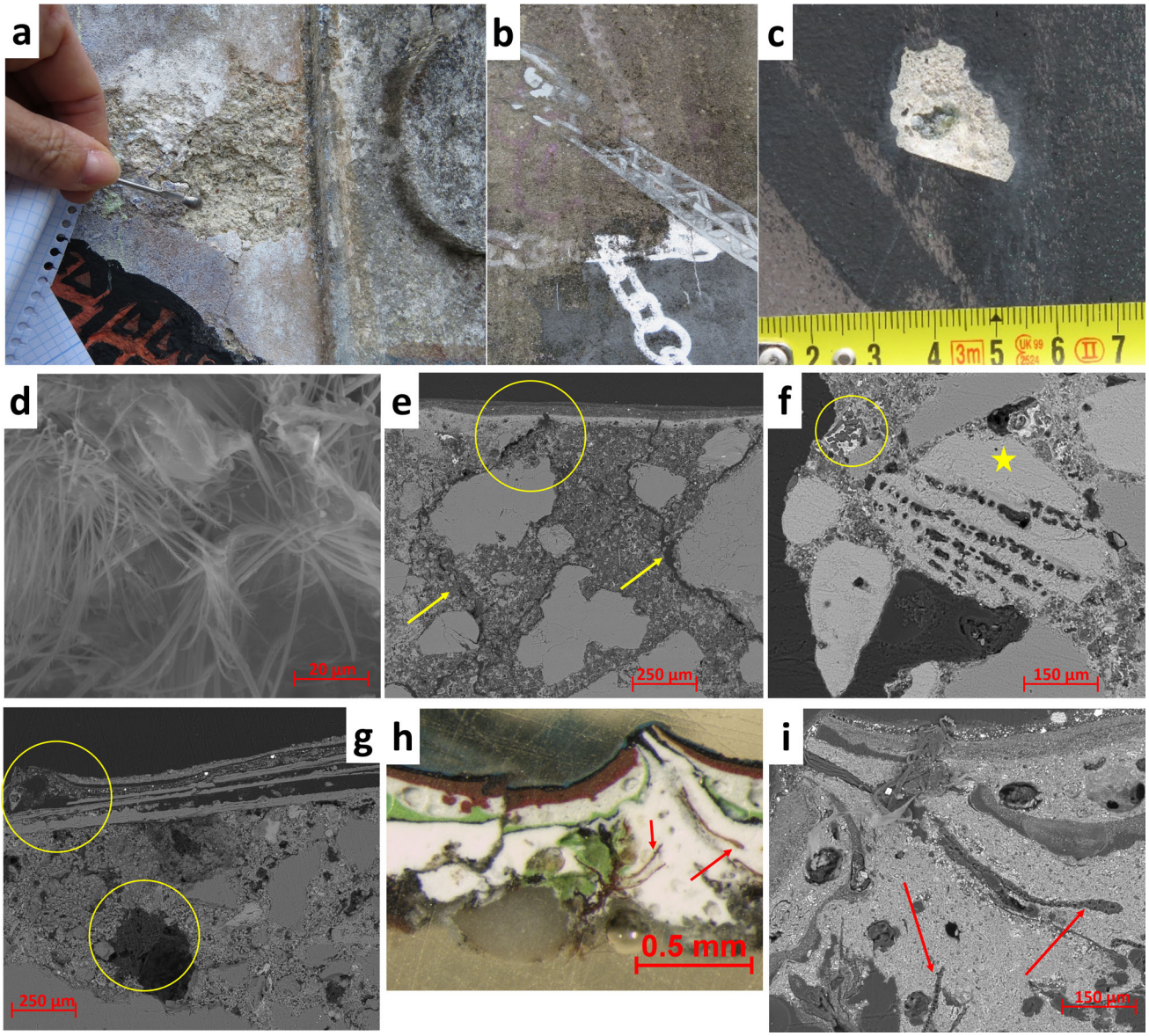

Fig. 5 Scaling affecting AW19 (**a**, of centimetre scale), AW17 (**b**, diffuse loss of millimetre scale) and AW20 (**c**, of centimetre scale); **d** SEM micrograph (SE mode) of the scaling sample depicted in **c**, in which ettringite fibres are distinguished; **e** SEM micrograph (BSE mode) of the cross section of a sample from AW19 of green painting on mortar affected by scaling; arrows indicate the transverse fissures and the circle indicates the limit between the fissure and the intact pictorial layer; **f** SEM micrograph (BSE mode) of the cross section of a sample from AW19 of green and yellow paintings on mortar affected by scaling; the asterisk indicates an aggregate grain of biogenic nature and the circle highlights an aggregate composed by residual non-hydrated cement phases (high contrast) and C–S–H phases (low contrast); **g** Micrograph taking with optic microscopy of a cross section of a sample from AW17 of white painting on mortar; the circles indicate the large pores filled with biological tissues that also appear under the detached paint layer; **h** and **i** micrographs of a sample from AW17 of blue painting on mortar taken under a stereoscopic microscope (**h**) and SEM (**i**; BSE mode); arrows point to growth structures of bryophytes, fungal hyphae and other organic tissues

whose relevance in the conservation of monuments located in coastal areas or in areas up to where the influence of the winds from the sea reaches has been reported by different authors [60, 61]. On the other hand, the presence of ettringite in the sample of reinforced concrete from AW19 confirmed that in this artwork, the formation of scaling is related to chemical deterioration by means of the sulphate reaction through the formation of secondary sulphates [52].

It appears that it is not only the action of salts that is related to the formation of scaling. Thus, in another artwork strongly affected by scaling, AW17 (Figs. 1a and 5b; painted on a brick wall coated with a cement-based render), SEM analysis of samples confirmed that the substrate had fissures and large pores (500 µm, Fig. 5g), which were filled with biological tissue. Mosses and fungal growth structures (hyphae), isolated cells and colonies of cells were observed (Fig. 5h, i); as can be seen in these micrographs, the organisms do not grow from the surface of the pictorial layer inwards, but rather the reverse occurs: they grow outwards from the substrate towards the pictorial layer. This indicates that the artwork was painted without prior thorough cleaning of the substrate. It

is important to note that this artwork (AW17, Fig. 1a) is painted on a wall that, because of its geographical orientation, is protected from sunlight and remains damp for long periods after rainfall. This situation favours colonization of the wall by diverse organisms. In fact, due to the temperate humid climate in Galicia, the surfaces of monuments are quickly colonized by various organisms [62, 63], so the conservation problem that biological colonization entails in architectural heritage [64, 65] acquires special relevance in this geographical area. Another finding confirming the lack of prior conditioning of the substrate is the identification of various layers of paint below the most recent layer and that originate from previous artworks (in Fig. 5g, h, note the existence of three layers of paint below the current pictorial layer). This was detected in both independent artworks (AW16 and AW17-Fig. 1a) and in commissioned ones (AW21-Fig. 1e).

(2) *Diffuse loss of material.* As already indicated, in some artworks a type of scaling that generated small gaps (millimetre-sized) in the paint surface, which we have defined as diffuse loss of the pictorial layer, was observed; artworks AW16 and AW17 (Figs. 1a, 5b and 6a) are representative of this type of deterioration. In the artworks affected, the areas in which diffuse loss of paint was identified remain damp for long periods (either because they are oriented to the N or because they are surrounded by buildings that act as screens) or are exposed to running water due to the absence of drainage systems in the structures. XRD analysis of samples affected by this type of alteration (Table 2, AW16 and AW17 samples) did not reveal the existence of exogenous mineral phases, such as salts, and only the mineral components of the paints (calcium carbonate, talc and rutile) and of the substrates (calcium carbonate and silicates, cement phase and aggregates, respectively) were detected. Examination of these samples by optic microscopy and SEM analysis confirmed the absence of salt and revealed strong biological activity: (1) in the aqueous preparations of the material scraped from the areas affected by diffuse loss of AW17 (Fig. 6a, b) cells of chlorophytes (green algae) (Fig. 6c) and colonies of cyanobacteria (Fig. 6d) were observed; (2) SEM analysis of the painted surfaces affected by this deterioration form confirmed an intense degree of biological colonization (Fig. 6e), distinguishing, on the surface of the painting, low contrast spots formed by compact tissues formed by interlaced hyphae and which may correspond to the mycelium of microscopic fungi, loose hyphae and chain-shaped colonies of cells—probably cyanobacteria (Fig. 6f). These observations would indicate that this type of alteration is caused by settlement on the paint surface of microorganisms whose growth, enhanced by the presence of water, leads to fragmentation and loss of the paint. Therefore, the important role of microscopic fungi, algae and cyanobacteria in the conservation of the materials used in pictorial urban art is confirmed, a role already firmly established in the conservation of ancient cultural heritage [64, 66].

In certain cases, biodeterioration may be active, but not visible to the human; thus, in areas of murals that are constantly damp, SEM analysis of areas in apparently good states of conservation confirmed the incipient biodeterioration. Figure 6g depicts the appearance, under the stereoscopic microscope, of a white painted area of the AW17 artwork that, to the naked eye, seemed to be intact. However, microscopic examination confirmed the presence of small black holes from which branching lines (possibly small cracks) arise. SEM analysis confirmed that the holes were filled with biological material and that they were connected with each other via hyphae and colonies of cells forming chains (probably *Nostocales* cyanobacteria of the genus *Scytonema*) (Fig. 6h). It is possible that these morphologies correspond to the initial stage of diffuse loss. The key importance of the presence of water in the development of this deterioration phenomenon is confirmed by the presence of large amounts of diatoms, which are common in freshwater surfaces (Fig. 6i).

(3) *Peeling.* The third type of alteration that leads to loss of the pictorial layer is peeling, in which the pictorial layer detaches cleanly from the substrate, sometimes after a bulge formation of the paint layer. Inspection of the artworks did not reveal any relationship between peeling and the orientation of the walls but did reveal a relationship with the type of substrate. Although detected in paintings on a large variety of materials, the artworks most strongly affected by peeling were those painted on brick, metal and unrendered reinforced concrete, being the best examples AW21 artwork (Figs. 2f–h and 6j–k), AW18 artwork and AW20 artwork (Fig. 7a). Monitoring of these three artworks over two years has shown that the peeling can occur shortly after completion of the artwork. Thus, in AW21 the peeling was obvious at 8 months after completion of the painting (compare Fig. 2f—photograph taken in 2018—and Fig. 2g—photograph taken in 2020). The following were also observed in this artwork: (1) the peeling was more intense and appeared at earlier stages on the surfaces of the original concrete (remember that, as indicated previously, the breakwater suffered a reconstruction in 2017 after a collapse provoked by a storm); in Fig. 6j, which shows an area with the original concrete and the reconstruction concrete, separated from each other by a joint, the peeling scarcely affected the area reconstructed in 2017, whereas, by contrast, the peeling is very intense in the original concrete; (2) the existence of a clear relationship between the intensity of the peeling and the type of paint. Thus, on the surface of the original concrete, peeling is particularly intense in areas painted with the base blue paint than, e.g. in areas painted with yellow paint (Fig. 2g–h). Conversely, peeling on surfaces of reconstructed concrete affected more intensely pink and light blue paintings, barely affecting the base blue paint (Fig. 6k).

The mineralogical composition of samples of peeling from AW21 (Fig. 1e) is shown in Table 2. In addition to the mineral phases expected to be found in paintings (calcite, rutile, talc—used as fillers or opacifiers), the following were detected: (1) silicate minerals such as quartz, feldspar and micas, present (in very small or trace amounts) due to contamination of the concrete substrate and (2) halite (NaCl) and sulphate salts, specifically epsomite [$MgSO_4 \cdot 7(H_2O)$] and thenardite (Na_2SO_4). Analysis of the soluble ion content of the peeling samples from this artwork revealed large quantities of chlorides and confirmed the presence of halite in the

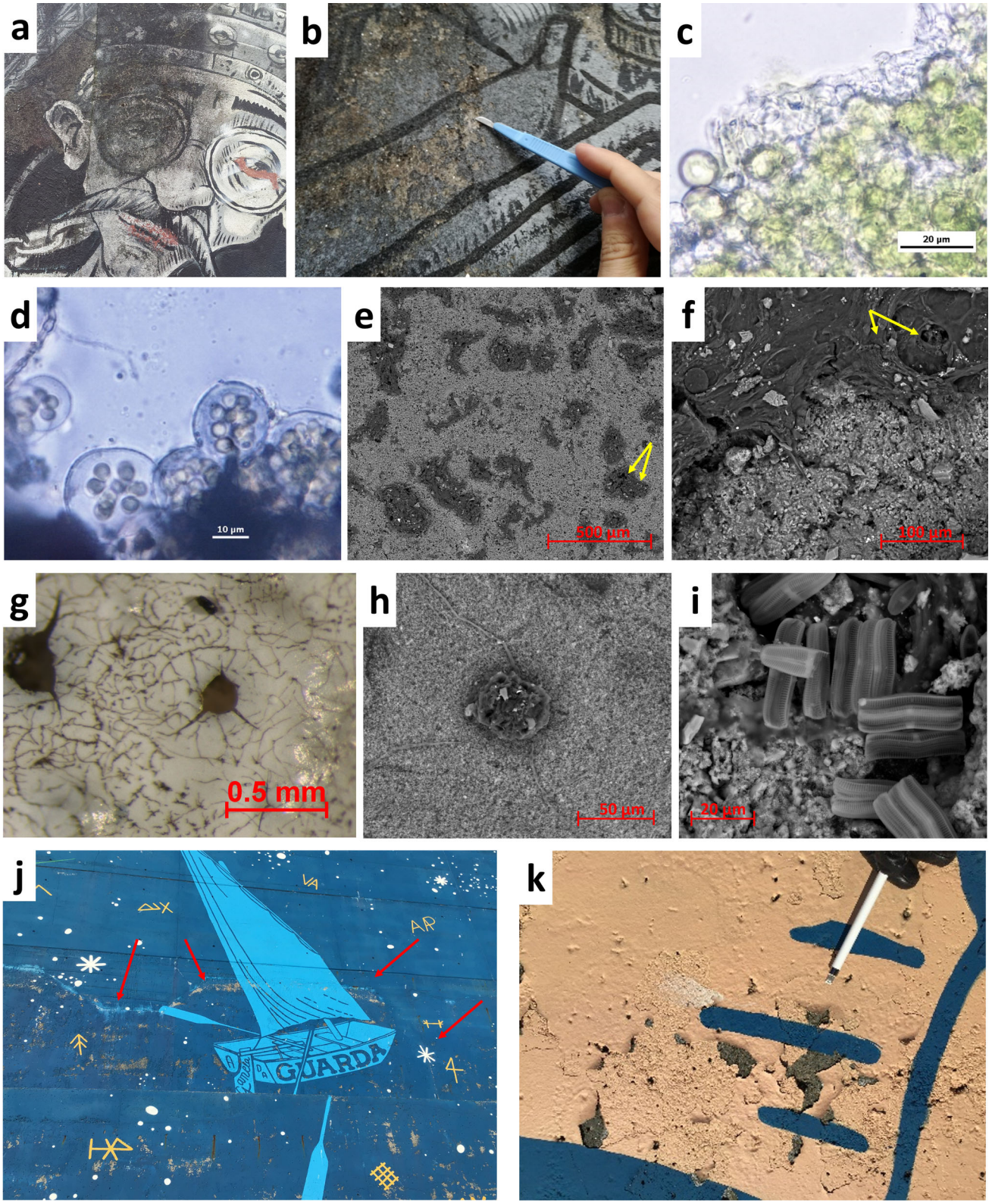

Fig. 6 **a**, **b** Diffuse loss of material affecting AW17; **c**, **d** micrographs taken with optic microscopy of surface material from an area affected by diffuse loss of AW17 where isolated cells of green algae (**c**) and colonies of cyanobacteria (**d**) are observed; **e** and **f** SEM micrographs (BSE mode) of the surface (**e**) and the cross section (**f**) of a painted surface affected by intense biological colonization; arrows point to biological tissues; **g–i** Micrographs of a simple of white paint from AW17 showing voids filled with biological tissues (**g**-stereoscopic microscopy and **h**-SEM, BS mode) and diatoms (**i**); **j** peeling affecting AW21; note that the intensity of the peeling affecting the original concrete is higher than that affecting the concrete of the breakwater reconstruction (the arrow marks the limit between both types of concrete); **k** peeling affecting pink-painted areas on AW21

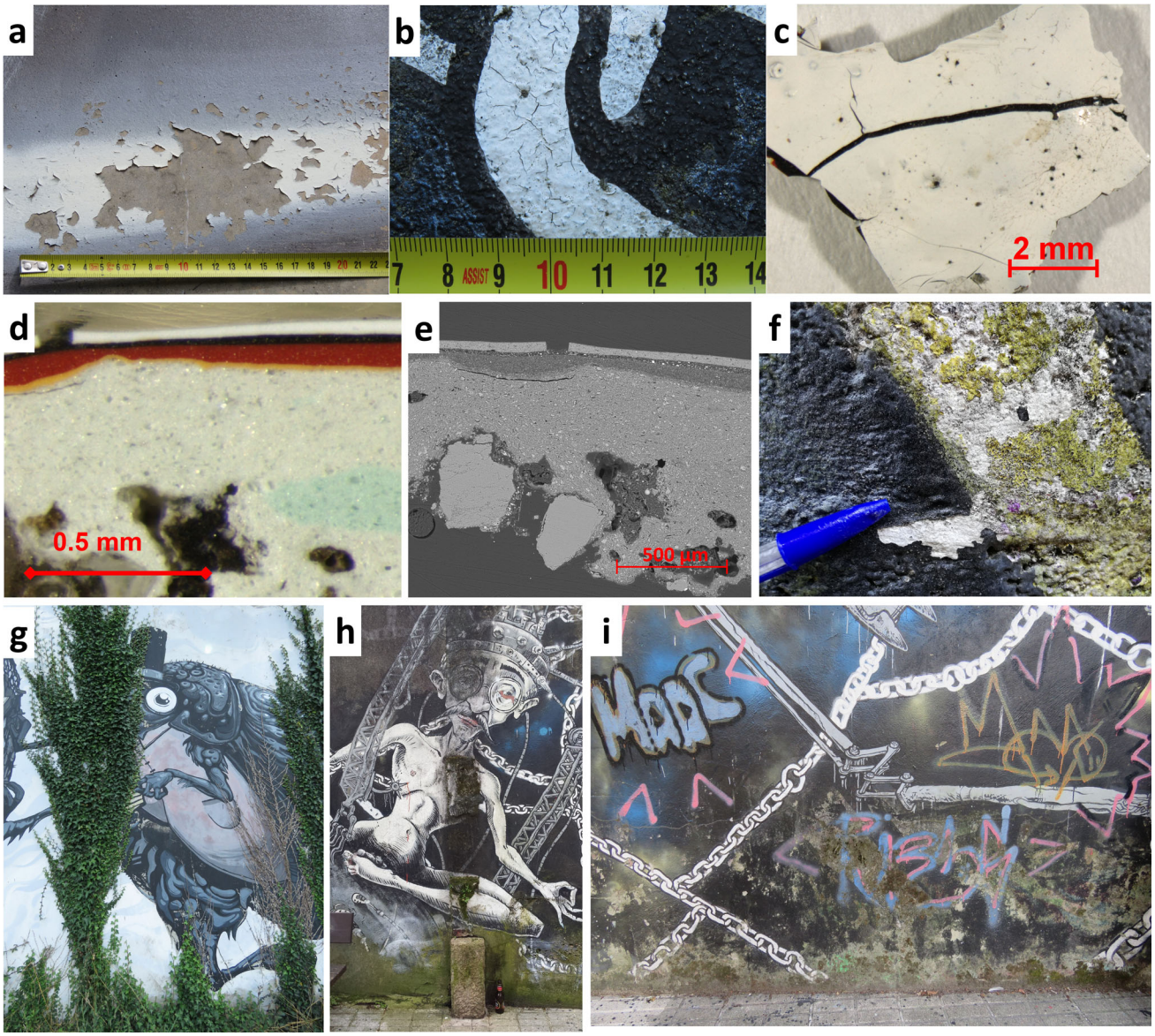

Fig. 7 **a** Peeling affecting AW20; **b** craquelure affecting white paintings on AW17; **c** micrograph of the surface of a craquelure sample from AW17; **d** and **e** micrographs of the cross section of the craquelure sample depicted in **c**, taken with optic microscopy (**d**) and SEM BSE mode (**e**); **f** biological colonization affecting AW16; **g** growing of vascular climbing plants on AW18; **h** biogenic black patina on AW17; **i** green patina, abrasion and vandalism on AW17

samples. The mineralogical composition and soluble ion content of samples of concrete substrates of AW 21 artwork is painted are also shown in Table 2: the original concrete (AW21-H1, Table 2), on which the peeling is more intense, and the more recent concrete, added during reconstruction in 2017 (AW21-H2, Table 2). These data confirmed, on the one hand, the different compositions of the two types of concrete: the recent concrete appears to be richer in cement phase than the original concrete, in accordance with observations made in situ, such as the smoother surface of the recent concrete. On the other hand, the extraction of soluble ions revealed much higher contents of chloride ions in the original concrete than in the recent one, in which the ion content is similar to that of the concrete in AW16, which is not affected by peeling. These findings appear to indicate that the peeling is due to crystallization of soluble salts at the paint-substrate interface; the alternating episodes of precipitation-dissolution at this interface would weaken the adherence and lead to loss of the pictorial layer. Soluble salts are considered among the most serious deterioration factors in the materials used in cultural heritage [67–71]; in ancient mural paintings, soluble salts are responsible both for the degradation of colour due to chemical alteration of pigments and for the physical loss of the paint layer due to the crystallization of salts in the form of efflorescence and sub-efflorescence [72–75]. In AW21 artwork, the original concrete of the breakwater has been in place for many years and the naturally high content of chloride ions (due to proximity to the sea) explains the more intense peeling in this material. However, peeling was also observed in the recent concrete, in which the salt content is lower, so there must be some other factor involved peeling formation. Taking into account previous works, this additional factor may be related to a weak adhesiveness

between the paint and the substrate. Alonso-Villar et al. [27], exposing mock-ups of the same paints applied on different substrates to UV radiation ageing tests, described the detachment of the pictorial layer from the substrate; this phenomenon occurred more intensely in paint samples applied on the smoother and more uniform substrate (brick). In AW21 artwork, the loss of adhesion between paint and substrate due to the exposure to the environment is expected to be more likely in the most recent concrete, because its smother surface. In this situation, salts from the environment will preferentially precipitate in the gap between paint and substrate since the larger the pore, the more probable is the crystallization of dissolved salts inside a porous material [76]; finally, the salt crystallization weakens the adherence between the two materials, favouring the detachment of the pictorial layer.

(4) *Craquelure*. Another manifestation of the deterioration affecting the integrity of the pictorial layer is craquelure, defined as a network of very fine cracks that specifically affect the pictorial layer and that eventually lead to loss of the layer. Craquelure was only detected in two of the artworks under study and, in one of these, only in some colours of paint: in AW20 (Fig. 2a) only the fluorescent orange was affected (Figs. 2a and 7a) and in AW17 (Fig. 1a) the white paint was affected (Fig. 7b). Examination of the samples by optic microscopy (Fig. 7c, d) and SEM (Fig. 7e) confirmed that the cracks only affect the surface layer of the painting, and there was no evidence that these fractures develop from the substrate. These observations appear to support the idea that the craquelure is due to failure related to shrinkage during polymer drying processes or to an excess of paint [77].

3.2.3 Biological colonization

Biological colonization was observed in almost all of the artworks under study, although the type and intensity of colonizing organisms depended on the orientation of the walls and locally on the presence of run-off water. Thus, in artworks exposed to solar radiation, biological colonization was limited to climbing plants growing up the walls (Fig. 7g) or vascular plants growing on parts of the artworks close to the ground. The impact caused by the growth of these vascular plants not only in the reading of the artwork but also in its conservation is clear; so, the need of controlling the growth of these organisms is confirmed, as occurs in ancient architectural heritage [78], by means the implementation of periodic maintenance measures. In the artworks where water accumulated, growth of lichens (Fig. 7f) and of biofilms were associated with run-off of water (Fig. 7h) or capillary rise, being responsible, as discussed previously, for diffuse loss of the pictorial layer.

3.2.4 Fissures, cracks (fractures)

These deterioration forms are defined as visible separation of material in two parts (from the pictorial layer or the substrate) via a rupture plane. These types of deterioration are clearly related to the substrate and are generally associated with the joints between different construction structures (pillars, masonry walls, eaves, footings, etc.). Thus, in party walls, the pictorial layer breaks via cracks associated with the joints between the brickwork and reinforced concrete pillars or structural bases forming part of the wall. In reinforced concrete walls, the discontinuities are associated with compaction defects or, in AW21 (Fig. 1e), with the borders between the original and the recent concrete.

3.2.5 Surface deposits

Salt efflorescences were identified in three artworks, AW13 and AW21 (Fig. 1e)—located beside the sea—and AW19, which, although located in an inland area, is sited beside a stream, as already mentioned. In AW13 and AW19 (Fig. 1b), the presence of salt efflorescences is associated with the previously described scaling; analysis of the samples of scaling from AW19 revealed the presence of gypsum and large amounts of sulphates (Table 2). In AW21, a few months after the artwork was completed, abundant surface deposits of an intense white colour appeared in cracks or discontinuities between the modular pre-cast concrete sheets (Fig. 2c–e) or at the joints between the original concrete and the reconstructed concrete (Fig. 6j). XRD analysis revealed that the deposits consist of calcium carbonate (Table 2) with traces of epsomite and thenardite; brucite ($Mg(OH)_2$) was also detected in another sample obtained from a fissure affected by infiltration of water. The presence of calcium carbonate in these deposits is symptomatic of the carbonation of portlandite ($Ca(OH)_2$) in the concrete, whereas the presence of brucite appears to indicate that the concrete of the breakwater is undergoing chemical attack related to the interaction between water rich in sulphate and magnesium (such as seawater) and the C–S–H components of concrete. It has been reported that, at the early stage of this type of chemical attack, a thin surface deposit of brucite forms due to the reaction between the magnesium ions and portlandite in the cement paste [79, 80]. Therefore, the concrete in AW21 would be undergoing the initial phase of this process. As portlandite was identified in the original concrete, this concrete would be undergoing the chemical attack, perhaps in the areas of contact with the reconstructed concrete where there will presumably be discontinuities through which seawater can seep. The absence of gypsum in either the types of concrete in the breakwater or in any of the samples of surface deposits confirms that the second stage of chemical attack, in which the calcium ions released in the previous stage react with sulphate to form gypsum [52] had not yet occurred.

The crystallization of these mineral phases in the surface deposits of AW21, especially of brucite, could be the reason of the whitening of the blue base paint of this artwork observed in areas close to cracks or discontinuities from which the deposits emerge (Figs. 2e and 6j). XRD analysis of the whitened areas of the blue base paint (Table 2) revealed the existence of a mixture of calcium

and magnesium carbonates, which were absent in the undeteriorated paint. This mixture of carbonates would be produced during carbonation of the portlandite in the presence of magnesium ions in solution.

3.2.6 Abrasion

It is defined as the loss of pictorial material (with or without the substrate) caused by rubbing or scraping with an object. This type of deterioration is very common in artworks that are accessible to the public, in which the abrasions are caused by impacts from objects, people or vehicles (Fig. 7i).

3.2.7 Vandalism

Any addition (graffiti, etching, stickers, etc.) that is not carried out by the author of the artwork is considered vandalism. This only affected four artworks accessible to the public: AW17 (Fig. 7i), AW16, AW19 and AW21.

4 Conclusions

The main conclusions about the deterioration affecting street art murals located in Galicia and selected for this study are as follows:

The artworks under study display specific types of deterioration determined by two key factors: the environment, on the one hand, and the intrinsic properties of the painting materials and the paint-substrate interaction, on the other.

The environment, specifically the availability of water and the existence of sources of soluble salts, determines the degradations that entail a physical loss of the paint layer. The growth of organisms (favoured by the presence of water) and the processes of crystallization-dissolution of salts, fundamentally of marine origin are the deterioration mechanisms implied in the deterioration forms that entail the physical loss of the pictorial layer. In the artworks affected by these deterioration forms, a clear influence of the geographical orientation and the proximity of salt sources with the intensity of the degradation can be confirmed. It is also important to point out that biodeterioration affects both non-commissioned works (whose substrates were never previously conditioned) and others recently created that have been promoted by local authorities; this finding highlights that large part of the deterioration issue of pictorial urban artwork in Galicia are closely related to the geographical area of study, where the temperate humid climate greatly conditions the durability of the materials, especially in regard to dampness and biological colonization. It would therefore be interesting to compare the results obtained with those of studies focused on artworks in drier climates.

The intrinsic properties of the painting materials and the paint-substrate interaction seem to be responsible for the other type of degradation of the studied urban artworks, which is fading, and which seems to be independent of environmental conditions (fundamentally geographical orientation and hours of sunlight). The intensity of fading appears to largely depend on the nature of the paint chromophores or the organic base that stabilizes the colour. The degree of insolation and the intensity of fading were not directly related, and the type of substrate did not affect the intensity of fading. Further study of the resistance of the paints most commonly used in urban art under controlled atmospheres and UV radiation should be carried out by applying the paint to different types of substrates in public spaces in order to identify the most resistant types of paint under different conditions. The information thus obtained would enable artists and authorities to prevent deterioration and increase the durability of the artworks.

In any case, the deterioration factors identified further increase the ephemeral nature of the urban artworks; however, when the artists and commissioning agents wish to prolong the durability of the artworks, the effects of some of these factors could easily be avoided by implementing preventive measures such as the following: (1) prior conditioning of the surface by applying lime mortar; (2) minimizing the effects of damp/water, by installing channelling and drainage systems; (3) evaluating the application of colour protectors; in this respect scientific studies of the effectiveness and durability of colour protectors under artificial ageing test are of great value, analysing the influence of the substrate and type of paint (the colour, the composition and the format—alkyd, polyester, spray, brush, etc.); (4) implementation of a periodic monitoring and control program for commissioned urban art with the aim of preventing deterioration of the artworks, especially focused on minimizing the biological colonization and the presence of damp (related to rainwater and seawater) and on in situ evaluate the durability of the pictorial materials.

It was also concluded that information obtained in interviews with the artists and through the dialogue established with this collective, the local authorities promoting many of the artworks and the paint manufacturers was essential for interpretation of some of the analytical data and correct diagnosis of the state of conservation of the artworks. Such information is of key importance and its diffusion among the public and authorities would help raise social awareness about these artistic expressions and thus favour their conservation.

This work is one of the first approaches towards the description of the particular deterioration forms of the materials used in contemporary murals under temperate climate and the identification of the main alteration factors involved. The information obtained supposes the necessary scientific foundation to carry out future diagnosis studies on murals under a similar climate. It would be

interesting to undertake similar studies applying different non-destructive techniques, in order to identify the most useful ones without sampling.

Acknowledgements This study was financed by the EU within the framework of the project CONSERVATION OF ART IN PUBLIC SPACES- CAPuS. E+ Knowledge Alliance KA2: Cooperation for innovation and the exchange of good practices, 2017-2021. Grant Agreement Number 2017 – 3674/001 – 001. E. M. Alonso-Villar contribution was supported by CAPuS project by a grant for mobility of research personnel from the University of Vigo (Axudas propias para a mobilidade de persoal investigador da Universidade de Vigo, 2021). J.S. Pozo-Antonio was supported by the Ministry of Science and Innovation, Government of Spain through grant number RYC2020-028902-I. XRD and SEM analyses were performed at the University of Vigo's Research Support Centre for Science and Technology (CACTI) and FTIR analyses at the University of Turin – Department of Chemistry. Thanks are given to Dr. Eugenia López de Silanes, from Universidade of Vigo, for her assistance in identifying colonizing organisms, to artists of the artworks studied for their involvement and to Ordes, Carballo, A Guarda and Vigo councils for support given to this project. Funding for open access charge: Universidade de Vigo/CISUG.

Author contributions Teresa Rivas contributed to conceptualization, investigation, resources, methodology, software; data curation, visualization, supervision, project administration, writing—original draft preparation, writing—reviewing, editing and funding acquisition. Enrique M. Alonso-Villar contributed to investigation, methodology, software, data curation and writing—original draft preparation. José S. Pozo-Antonio contributed to conceptualization, investigation, resources, methodology, supervision, project administration, writing—reviewing, editing and funding acquisition.

Funding Open Access funding provided thanks to the CRUE-CSIC agreement with Springer Nature.

Data Availability Statement This manuscript has associated data in a data repository. [Author's comment: Data associated with the present work and other investigations related to the CAPuS Project can be found at https://www.capusrepository.unito.it/].

Declarations

Conflict of interest The authors declare that they have no known competing financial interests or personal relationships that could have appeared to influence the work reported in this paper.

References

1. P. Mora, *Causes of Deterioration of Mural Paintings* (ICCROM publications, 1974), pp. 74
2. S. Siegesmund, T. Weiss, A. Vollbrecht, Geol. Soc. Lond. **205**(1), 1 (2002). https://doi.org/10.1144/GSL.SP.2002.205.01.01
3. ICOMOS-ISCS, *Illustrated Glossary on Stone Deterioration Patterns. Glossaire illustré sur les formes d'altération de la pierre* (ICOMOS International Scientific Committee for Stone (ISCS) Champigny/Marne, France, 2008). ISBN: 978-2-918086-00-0. EAN: 9782918086000
4. EwaGlos, *European Illustrated Glossary of Conservation Terms for Wall Paintings and Architectural Surfaces* (Michael Imhof Verlag, Petersberg, Germany, 2015), p. 448. ISBN: 978-3-7319-0260-7. https://doi.org/10.5165/hawk-hhg/234
5. C. Soffritti, L. Calzolari, A. Balbo, F. Zanotto, C. Monticelli, A. Fortini, G.L. Garagnani, Metall. Ital. **4**, 5 (2018)
6. C. Soffritti, L. Calzolari, A. Balbo, F. Zanotto, C. Monticelli, A. Fortini, G.L. Garagnani, Eur. Phys. J. Plus **134**, 424 (2019). https://doi.org/10.1140/epjp/i2019-12944-y
7. S.M. Sunara, N. Peko, I. Miletić Čakširan, Stud. Conserv. **63**(sup1), 428 (2018). https://doi.org/10.1080/00393630.2018.1486080
8. A. Bosi, A. Ciccola, I. Serafini, M. Guiso, F. Ripanti, P. Postorino, R. Curini, A. Bianco, Spectrochim. Acta A Mol. Biomol. Spectrosc. **225**, 117474 (2020). https://doi.org/10.1016/j.saa.2019.117474
9. J. La Nasa, S. Orsini, I. Degano, A. Rava, F. Modugno, M.P. Colombini, Microchem. J. **124**, 940 (2016). https://doi.org/10.1016/j.microc.2015.06.003
10. J. La Nasa, B. Campanella, F. Sabatini, A. Rava, W. Shank, P. Lucero-Gomez, D. De Luca, S. Legnaioli, V. Palleschi, M.P. Colombini, I. Degano, F. Modugno, J. Cult. Herit. **48**, 129 (2021). https://doi.org/10.1016/j.culher.2020.11.016
11. A. Rousaki, P. Vandenabeele, M. Berzioli, I. Saccani, L. Fornasini, D. Bersani, Eur. Phys. J. Plus. **137**, 252 (2022). https://doi.org/10.1140/epjp/s13360-022-02423-1
12. D. Cimino, R. Lamuraglia, I. Saccani, M. Berzioli, F.C. Izzo, Heritage **5**, 581 (2022). https://doi.org/10.3390/heritage5020033
13. E. Gayo, Ge-Conservacion **10**, 97 (2016). https://doi.org/10.37558/gec.v10i0.401
14. R. Schacter, Street Art Is a Period. (Hyperallergic, July 2016). https://hyperallergic.com/310616/street-art-is-a-period-period-or-the-emergence-of-intermural-art/. Accessed 28 April 2022.
15. J. Abarca, Str. Art Urban Creat. **3**(2), 112 (2017). https://doi.org/10.25765/sauc.v3i2.87
16. M. Chatzidakis, *Preventive Conservation and Monitoring of Street Art, Graffiti, and Public Murals: Education and Training as an Effective Tool*. Conference Paper Spanish Group (GEIIC) of the International Institute of Conservation (IIC), ed. by Grupo Español del IIC (Vitoria-Gasteiz, Spain, 2018), pp. 96–105. ISBN 9788409051779.
17. A.L. Mata Delgado, *Conservando street art & graffitti. Pertinencia de su conservación y problemática material derivada de su técnica de manufactura, X Foro Académico Restauración, la indisciplina en práctica* (Guadalajara, Jalisco, México, 2013)
18. E. Gayo, Str. Art Urban Creat. **3**(1), 26 (2017). https://doi.org/10.25765/sauc.v3i1.60
19. E. Gayo, *Conservación de arte urbano. Vermibus, de la calle al estudio y la galería*, 19ª jornada sobre Conservación de arte contemporáneo (Museo Nacional Centro de Arte reina Sofía, Madrid, 2018), p. 277

20. C. Santabárbara, Opus Quad. Di Stor. Archit. Restauro Disegno=journal Hist. Archit. Conserv. Draw. Nuova Ser. **2**, 147 (2018). https://doi.org/10.36165/2147
21. T. Learner, *Analysis of Modern Paints* (GCI Publications, 2005), p. 210. ISBN: 0892367792 9780892367795.
22. D. Scalarone, O. Chiantore, T. Learner, Ageing studies of acrylic emulsion paint, part II: comparing formulations with poly (EA-co-MMA) and poly (n-BA-co-MMA) binders (James & James, 2005), p. 850. ISBN: 1-902916-30-1.
23. M.T. Doménech-Carbó, M.F. Silva, E. Aura-Castro, L. Fuster-López, S. Kröner, M.L. Martínez-Bazán, X. Más-Barberá, M.F. Meeklenburg, L. Osete-Cortina, A. Doménech, J.V. Gimeno-Adelantado, D.J. Yusá-Marco, Anal. Bioanal. Chem. **399**(9), 2921 (2011). https://doi.org/10.1007/s00216-010-4294-3
24. V. Pintus, S. Wei, M. Schreiner, Microchem. J. **124**, 949 (2016). https://doi.org/10.1016/j.microc.2015.07.009
25. A. Ciccola, M. Guiso, F. Domenici, F. Sciubba, A. Bianco, Polym. Degrad. Stab. **140**, 74 (2017). https://doi.org/10.1016/j.polymdegradstab.2017.04.004
26. M. Bertasa, C. Ricci, A. Scarcella, F. Zenucchini, G. Pellis, P. Croveri, D. Scalarone, Coatings **10**(11), 1019 (2020). https://doi.org/10.3390/coatings10111019
27. E.M. Alonso-Villar, T. Rivas, J.S. Pozo-Antonio, Prog. Org. Coat. **154**, 106180 (2021). https://doi.org/10.1016/j.porgcoat.2021.106180
28. J.S. Pozo-Antonio, T. Rivas, N. González, E.M. Alonso-Villar, Sci. Total Environ. **826**, 154169 (2022). https://doi.org/10.1016/j.scitotenv.2022.154169
29. CAPuS project. http://www.capusproject.eu/. Accessed 26 April 2022
30. Glossary – CAPuS. https://capusproject.eu/glossary/. Accessed 26 April 2022
31. L. Romaní Fernández, Mecanismos de transformación de la idea de arte público. Experiencia y experimentación en el contexto gallego, Doctoral Thesis (Universidade de Vigo, 2012).
32. L. Arévalo Iglesias, Hist Comun Soc. **19**, 565 (2014). ISSN: 1137-0734. https://doi.org/10.5209/rev_HICS.2014.v19.44985
33. S. Cotte, N. Tse, A. Inglis, AICCM Bull. **37**(2), 107 (2016). https://doi.org/10.1080/10344233.2016.1251669
34. M.I. Úbeda García, Ge-conservacion **10**, 169 (2016). ISSN: 1989–8568. https://doi.org/10.37558/gec.v10i0.410
35. CIE S014-4/E:2007, *Colorimetry Part 4: CIE 1976 L*a*b* Colour Space* (CIE Central Bureau, Vienna, 2007)
36. A. Martínez-Cortizas, An. Edafol. Agrobiol. **46**, 521 (1987)
37. A. Martínez-Cortizas, A. Pérez, *Atlas Climático de Galicia* (Xunta de Galicia, 1999). ISBN: 84-453-2611-2
38. M. Kottek, J. Grieser, C. Beck, B. Rudolf, F. Rubel, Meteorol. Z. **15**, 259 (2006). https://doi.org/10.1127/0941-2948/2006/0130
39. W. Mokrzycki, M. Tatol, Color difference DeltaE-A survey, Mach. Graph. Vis. **20**, 383 (2011). https://www.researchgate.net/publication/236023905_Color_difference_Delta_E_-_A_survey
40. G. Socrates, *Infrared and Raman Characteristic Group Frequencies: Tables and Charts,* 3rd edn. (John Wiley and Sons, 2001). https://doi.org/10.1021/ja0153520
41. S.M. Cakić, I.S. Ristić, J.M. Vladislav, J.V. Stamenković, D.T. Stojiljković, Prog. Org. Coat. **73**, 401 (2012). https://doi.org/10.1016/j.porgcoat.2010.12.002
42. O. Chiantore, L. Trossarelli, M. Lazzari, Polymer **41**, 1657 (2000). https://doi.org/10.1016/S0032-3861(99)00349-3
43. O. Chiantore, M. Lazzari, Polymer **42**, 17 (2001). https://doi.org/10.1016/S0032-3861(00)00327-X
44. C. Duce, C.V. Della Porta, M.R. Tiné, A. Spepi, L. Ghezzi, M.E. Colombini, E. Bramanti, Spectrochim. Acta A Mol. Biomol. Spectrosc. **130**, 214 (2014). https://doi.org/10.1016/j.saa.2014.03.123
45. R. Ploeger, D. Scalarone, O. Chiantore, J. Cult. Herit. **9**, 412 (2008). https://doi.org/10.1016/j.culher.2008.01.007
46. P.M. Whitmore, V.G. Colaluca, Stud. Conserv. **40**(1), 51 (1995). https://doi.org/10.2307/1506611
47. R. Lambourne, T.A. Strivens, *Paint and Surface Coatings. Theory and Practice*, 2nd edn. (Woodhead Publishing Ltd, Abington Hall, Cambridge, 1999). ISBN: 978-1-85573-348-0. https://doi.org/10.1533/9781855737006
48. M.J. Melo, S. Bracci, M. Camaiti, O. Chiantore, F. Piancenti, Polym. Degrad. Stab. **66**, 23 (1999). https://doi.org/10.1016/S0141-3910(99)00048-8
49. D. Feldman, J. Polym. Environ. **10**, 163 (2002). https://doi.org/10.1023/A:1021148205366
50. T. Learner, O. Chiantore, D. Scalarone, *Ageing Studies of Acrylic Emulsion Paints* (James & James, London, 2002). ISBN: 1-902916-30-1
51. A. Cogulet, P. Balnchet, V. Labdry, Coatings **9**, 121 (2019). https://doi.org/10.3390/coatings9020121
52. M. Santhanam, M.D. Cohen, J. Olek, Cem. Concr. Res. **33**, 341 (2003). https://doi.org/10.1016/S0008-8846(02)00958-4
53. B. Silva Hermo, B. Prieto Lamas, T. Rivas Brea, L. Pereira Pardo, Mater. Constr. **60**, 297 (2010). https://doi.org/10.3989/mc.2010.46808
54. T. Rivas, S. Pozo, M. Paz, Sci. Total Environ. **482–483**, 137–147 (2014). https://doi.org/10.1016/j.scitotenv.2014.02.128
55. B. Silva, T. Rivas, E. García-Rodeja, B. Prieto, Atmos. Environ. **41**, 4396–4407 (2007). https://doi.org/10.1016/j.atmosenv.2007.01.045
56. S. Diamond, Cem. Concr. Compos. **26**, 919 (2004). https://doi.org/10.1016/j.cemconcomp.2004.02.028
57. G. Gosselin, V. Verges-Belmin, A. Royer, G. Martinet, Mater. Struct. **42**, 749 (2009). https://doi.org/10.1617/s11527-008-9421-7
58. A.M. Neville, *Properties of Concrete*, 5th edn. (Pearson, Harlow, 2011). ISBN-10: 0273755803. ISBN-13: 9780273755807
59. M. Jedidi, O. Benjeddou, MOJ Civil Eng. **4**(1), 40 (2018). https://doi.org/10.15406/mojce.2018.04.00095
60. F. Zezza, F. Macrì, Sci. Total Environ. **167**(1–3), 123 (1935)
61. H. Morillas, M. Maguregui, E. Gallego-Cartagena, I. Marcaida, N. Carral, J.M. Madariaga, Sci. Total Environ. **745**, 140899 (2020). https://doi.org/10.1016/j.scitotenv.2020.140899
62. B. Prieto Lamas, M.T. Rivas Brea, B.M. Silva Hermo, Sci. Total Environ. **167**, 343 (1995)
63. B. Silva, B. Prieto, T. Rivas, M.J. Sánchez-Biezma, G. Paz, R. Carballal, Int. Biodeterior. Biodegrad. **40**(2–4), 263 (1997). https://doi.org/10.1016/S0964-8305(97)00051-6
64. T. Warscheid, J. Braams, Int. Biodeterior. Biodegrad. **46**, 343 (2000)
65. G. Ranalli, E. Zanardini, C. Sorlini, *Encyclopedia of Microbiology*, 3rd edn (Academic Press, 2009), pp. 191–205. ISBN 9780123739445. https://doi.org/10.1016/B978-012373944-5.00132-2
66. K.L. Garg, K.K. Jain, A.K. Mishra, Sci. Total Environ. **167**(1–3), 255 (1995), ISSN: 0048-9697. https://doi.org/10.1016/0048-9697(95)04587-Q
67. A. Arnold, in *Dessalement des Matériaux Poreux: 7èmes journées d'études de la SFIIC* (Poitiers, 1996), pp. 3–20.
68. A.E. Charola, J. Am. Inst. Conserv. **39**, 327 (2000). https://doi.org/10.1179/019713600806113176
69. E. Doehne, Geol. Soc. Lond. **205**, 51 (2002). https://doi.org/10.1144/GSL.SP.2002.205.01.05
70. B. Silva, T. Rivas, B. Prieto, 2003 in *Applied Study of Cultural Heritage and Clays*, ed. by J.L. Pérez (Consejo Superior de investigaciones científicas, Madrid, 2003), pp. 113–130.
71. M. Steiger, Restor. Build. Monum. **11**(6), 419 (2005). https://doi.org/10.1515/rbm-2005-6002
72. J. Weber, in *Conservation of Architectural Surfaces: Stone and Wall Coverings*, ed. by G. Bisconti, L. Graziano (Il Cardo, Venezia, 1993), pp. 97–103.
73. K. Zehnder, 1996, in *Proceedings 8th International Congress on Deterioration and Conservation of Stone*. ed. by J. Riederer (Möller Druck, Berlin, 1996), pp.1669–1678

74. H. Leitner, Restor. Build. Monum. **11**(6), 365 (2005). https://doi.org/10.1515/rbm-2005-5998
75. S. Sfarra, C. Ibarra-Castanedo, M. Tortora, L. Arrizza, G. Cerichelli, I. Nardi, X. Maldague, J. Cult. Herit. **18**, 229 (2016). ISSN 1296-2074. https://doi.org/10.1016/j.culher.2015.07.011
76. G.W. Scherer, Cem. Concr. Res. **29**, 1347 (1999). https://doi.org/10.1016/S0008-8846(99)00002-2
77. D.G. Weldon, *Failure Analysis of Paints and Coatings* (John Wiley & Sons, 2009). https://doi.org/10.1002/9780470744673
78. A.K. Mishra, K.K. Jain, K.L. Garg, Sci. Total Environ. **167**, 375 (1995). https://doi.org/10.1016/0048-9697(95)04597-T
79. D. Bonen, M.D. Cohen, Cem. Concr. Res. **22**, 169 (1992). https://doi.org/10.1016/0008-8846(92)90147-N
80. D. Bonen, M.D. Cohen, Cem. Concr. Res. **22**, 707 (1992). https://doi.org/10.1016/0008-8846(92)90023-O